

# Large voltage-induced magnetic anisotropy change in a few atomic layers of iron

T. Maruyama<sup>1</sup>, Y. Shiota<sup>1</sup>, T. Nozaki<sup>1</sup>, K. Ohta<sup>1</sup>, N. Toda<sup>1</sup>, M. Mizuguchi<sup>1†</sup>, A. A. Tulapurkar<sup>1</sup>, T. Shinjo<sup>1</sup>, M. Shiraishi<sup>1</sup>, S. Mizukami<sup>2</sup>, Y. Ando<sup>3</sup> and Y. Suzuki<sup>1\*</sup>

**In the field of spintronics, researchers have manipulated magnetization using spin-polarized currents<sup>1–3</sup>. Another option is to use a voltage-induced symmetry change in a ferromagnetic material to cause changes in magnetization or in magnetic anisotropy<sup>4–14</sup>. However, a significant improvement in efficiency is needed before this approach can be used in memory devices with ultralow power consumption. Here, we show that a relatively small electric field (less than 100 mV nm<sup>−1</sup>) can cause a large change (~40%) in the magnetic anisotropy of a bcc Fe(001)/MgO(001) junction. The effect is tentatively attributed to the change in the relative occupation of 3d orbitals of Fe atoms adjacent to the MgO barrier. Simulations confirm that voltage-controlled magnetization switching in magnetic tunnel junctions is possible using the anisotropy change demonstrated here, which could be of use in the development of low-power logic devices and non-volatile memory cells.**

To develop voltage-driven spintronic devices, several areas of investigation have been suggested, including voltage control of magnetic anisotropy<sup>4,7</sup>, ferromagnetism in ferromagnetic semiconductors<sup>8,9</sup>, magnetoelectric switching of exchange bias<sup>10,11</sup> and anisotropy<sup>12</sup>, magnetoelectric interface effects<sup>5,6</sup>, multiferroic properties<sup>13</sup> and magnetostriction in a hybrid system with piezoelectric materials<sup>14</sup>. Most work to date has been carried out only at low temperatures, using GaMnAs or perovskite systems, or needed piezoelectric distortions, which may limit the endurance of any devices. Weisheit and colleagues<sup>7</sup> observed up to 4.5% coercivity change in FePt(Pd) films with the application of voltage. However, they required the use of a liquid electrolyte to apply a high electric field at the surface. In this study, we have overcome these difficulties by using ultrathin Fe/MgO junctions. The system is built from all-solid-state and distortion-free materials that have controllable perpendicular surface anisotropy<sup>15–20</sup>.

As shown in Fig. 1, the sample structure stack layers comprised a MgO substrate/MgO(10 nm)/Cr(10 nm)/Au(50 nm)/Fe(2–4 ML)/MgO(10 nm)/polyimide(1,500 nm)/ITO(100 nm) (ML, monatomic layer; see Methods). Because the influence of the electric field on the perpendicular anisotropy is effective only at the interface, the ferromagnetic layer had to be composed of only a few monatomic layers. In addition, to control the perpendicular anisotropy, the film had to have a moderate crystalline and surface anisotropy in the absence of the bias voltage. In this regard, we used an ultrathin Fe layer for the anisotropy change. Because the Fe grew almost in a layer-by-layer mode onto the Au(001) surface at room temperature, we were able to precisely control the layer thickness<sup>21</sup>. The ultrathin epitaxial Fe layer deposited on the Au(001) buffer layer exhibited a transition in magnetic anisotropy from in-plane to perpendicular, depending on

the film thickness<sup>20</sup>. Such features are ideal for the observation of the anisotropy change in response to the electric field, because we could systematically control the strength of the perpendicular anisotropy. The insulating layers comprised MgO and polyimide. MgO was used because it can be epitaxially grown onto an Fe(001) surface and exhibits a high breakdown voltage as a barrier material in magnetic tunnel junctions<sup>22</sup>. The polyimide layer was used to ensure a pinhole-free barrier over an extended area.

Figure 2 shows representative magnetic hysteresis loops in a 0.48-nm-thick Fe layer under the application of a bias voltage, obtained from Kerr ellipticity,  $\eta_K$ , measurements. Under two different bias voltages,  $U = +200$  and  $-200$  V, a significant change in perpendicular anisotropy was observed. The perpendicular magnetic anisotropy energy per unit volume of the film,  $E_{\text{perp}}$ , was calculated from the  $\eta_K$ - $H$  curve, assuming a linear relation between  $\eta_K$  and magnetization:

$$E_{\text{perp}} = -\mu_0 \frac{M_s}{\eta_s} \int_0^{\eta_s} H d\eta_K, \quad (1)$$

where  $\mu_0$ ,  $M_s$ ,  $H$ ,  $\eta_K$  and  $\eta_s$  are permeability of free space, saturation magnetization, external magnetic field, Kerr ellipticity and saturation Kerr ellipticity, respectively. If the film possesses uniaxial crystalline anisotropy  $K_u$ , and surface anisotropy  $K_s$ , the  $E_{\text{perp}}$  is expressed as

$$E_{\text{perp}} d = \left( -\frac{1}{2} \mu_0 M_s^2 + K_u \right) d + K_{s,\text{MgO/Fe}} + K_{s,\text{Fe/Au}} + \Delta K_s(V) \quad (2)$$

where  $d$  is the film thickness.  $\Delta K_s(V)$  is a surface anisotropy, induced by application of a voltage. When a positive voltage  $U = +200$  V was applied, then decreased to  $U = -200$  V, perpendicular anisotropy was induced and the magnetic anisotropy energy was changed from  $-31.3$  to  $-13.7$  kJ m<sup>−3</sup>. The ratio of the magnetic anisotropy energy change, defined as  $\Delta E_{\text{perp}} / (2E_{\text{perp,ave}}) = (E_{\text{perp,200V}} - E_{\text{perp,-200V}}) / (E_{\text{perp,200V}} + E_{\text{perp,-200V}})$ , was 39%. If we count this change as a change in the surface anisotropy energy, that is,  $\Delta K_s(V)$  in equation (2), it corresponds to 8.4  $\mu\text{J m}^{-2}$ .

To precisely measure the thickness dependence of the effect, we used a modulation technique (see Methods). The inset in Fig. 2 shows the external field dependence of the  $d\eta_K/dV$  signal that was obtained for the same sample. The  $d\eta_K/dV$  signal displays a maximum value,  $(d\eta_K/dV)_{\text{max}}$ , where the  $\eta_K$  hysteresis curves, obtained for positive (B) and negative (A) bias voltages, show a

<sup>1</sup>Graduate School of Engineering Science, Osaka University, Toyonaka, Japan; <sup>2</sup>WPI Advanced Institute for Materials Research, Tohoku University, Sendai, Japan; <sup>3</sup>Graduate School of Engineering, Tohoku University, Sendai, Japan; <sup>†</sup>Present address: Institute for Materials Research, Tohoku University, Sendai, Japan; \*e-mail: suzuki-y@mp.es.osaka-u.ac.jp

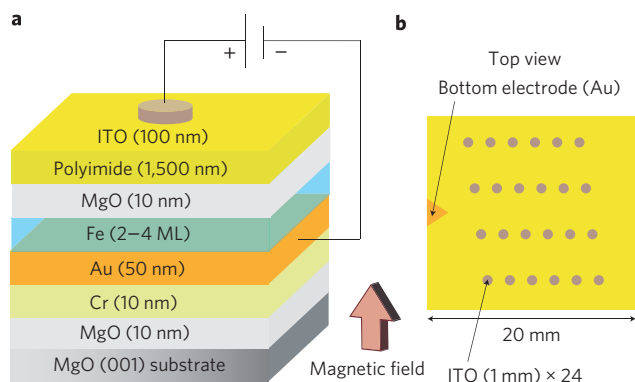


**Figure 1 | Schematic of the sample used for a voltage-induced magnetic anisotropy change.** **a**, A positive voltage is defined as a positive voltage on the top electrode with respect to the bottom electrode. A perpendicular magnetic anisotropy was induced by a negative voltage. The magnetic field was applied perpendicular to the film plane for Kerr ellipticity measurements. **b**, We fabricated the wedge-shaped Fe layer, incorporating 24 samples on the substrate, to investigate the dependence of the effect on Fe thickness.

maximum difference (C point in Fig. 2, inset). Figure 3a shows  $(d\eta_K/dV)_{\max}$  as a function of film thickness. The effect was largest for an Fe film with a thickness of 0.48 nm, and was smaller for both thinner and thicker films. Because the influence of the electric field is effective only at the metal/insulator interface, it is natural to observe a smaller effect for the thicker Fe films. Figure 3b shows the dependence of the saturation Kerr ellipticity,  $\eta_s$ , on Fe thickness. The linear dependence of  $\eta_s$  down to 0.25 nm (1.8 ML on average) proves that continuous films had been grown, even if they were only a few atomic layers in thickness. In addition, this behaviour also proves that the film was uniform across the thickness. In Fig. 3c,  $E_{\text{perp}}d$  is plotted as a function of Fe layer thickness  $d$  at zero bias voltage, together with a linear fit using equation (2). The fit indicates that  $K_{s,\text{MgO/Fe}} + K_{s,\text{Fe/Au}} = 580 \mu\text{J m}^{-2}$  and  $M_s = 1.5 \text{ MA m}^{-1}$ , neglecting a contribution from  $K_u$ .  $M_s$  is about 83% that of the bulk value. The reduction in the apparent  $M_s$  could be caused by a contribution from a positive  $K_u$ , produced by a lattice mismatch between Fe and Au (1.6%). The value of  $K_{s,\text{MgO/Fe}} + K_{s,\text{Fe/Au}}$  observed here was a little higher than previous observations made on a Au/Fe(001) interface<sup>23</sup>,  $K_{s,\text{Fe/Au}} = 470, 400, 540 \mu\text{J m}^{-2}$ . This suggests that the MgO/Fe interface also has a positive contribution to  $K_s$ . The experimental data deviate from the linear fit line below 0.48 nm. This is well-documented behaviour for ultrathin films and may have many origins<sup>24</sup>. The thickness at which the linear fit, using equation (2), starts to deviate corresponds to the thickness where the maximum of  $(d\eta_K/dV)_{\max}$  is obtained. One of the possible reasons for this is a deterioration of the film quality in this ultrathin thickness region. Clarification of the mechanism of the deviation requires further investigation.

One possible origin of the effect is in the influence of an electric field on electron filling of the Fe layer, which should affect the magnetic anisotropy (see Supplementary Information). Kyuno and colleagues pointed out that surface magnetic anisotropies in 3d ferromagnetic metal/noble metal interfaces were very sensitive to the electron filling of 3d orbitals<sup>25</sup>. In our case, from the capacitance of the junction, we estimate that we could change electron filling by  $2 \times 10^{-3}$  electrons per Fe surface atom by the application of 200 V. From the density of states, this corresponds to about 1 meV change in chemical potential (see Supplementary Information). This small change, however, may produce a non-negligible change in the surface anisotropy energy. From our experiment, we could change anisotropy energy by 4  $\mu\text{eV}$  per surface Fe atom. This magnitude

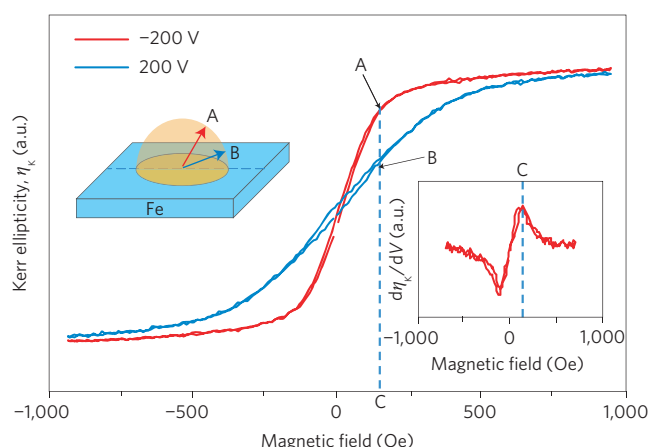


**Figure 2 | Magneto-optical Kerr ellipticity  $\eta_K$  for different applied voltages as a function of applied field.** The thickness of the Fe film was 0.48 nm.

A significant change in the hysteresis curve indicated a large change in perpendicular anisotropy following application of the bias voltage. The right inset shows the voltage modulation response of the Kerr ellipticity,  $d\eta_K/dV$ . The left inset illustrates the magnetization direction at points A and B in the hysteresis curves.

of change can be reproduced from Kyuno's calculation using 1 meV change in the chemical potential. Kyuno also noted that the effect originates mainly from the large density of states (DOS) of a  $d_{xy}$  and  $d_{x^2-y^2}$  character ( $|m_z| = 2$ ) in the Fermi energy in the Fe/Au (001) system, in which Au has a large spin-orbit coupling<sup>26–29</sup>. In our case, because the Fe has two interfaces, with Au(001) and MgO(001), the situation is not completely the same, but a similar mechanism may occur. As schematically shown in Fig. 3d, the application of a negative voltage, for example, may cause an increase in the energy of the  $d_{3z^2-r^2}$  ( $m_z = 0$ ) states, because of higher electron density at the barrier/Fe interface, leading to a reduction in the electron occupancy in those states. Therefore, the electron occupancy in the  $d_{xy}$  and  $d_{x^2-y^2}$  states could be changed relative to one another, leading to a modulation of the magnetic anisotropy. Further discussion requires first principles calculations.

In our experiment, we needed to apply a large voltage because of the thickness of the polyimide layer. The estimated voltage drop across the MgO layer, however, was  $\sim 45 \text{ mV nm}^{-1}$  if we can neglect charge accumulation in the barrier (see Supplementary Information). As we know that more than 2 V can be applied to a 2-nm-thick MgO barrier, a much larger effect can be expected for conventional tunnel magnetoresistance junctions with a MgO barrier.

In the latter part of this letter, we suggest a novel magnetization switching technique, using the voltage-induced magnetic anisotropy change explored in this work (see Supplementary Information). Figure 4 shows a result of macro-spin model simulation of voltage-controlled magnetization switching for a 0.48-nm Fe film. Here, we used parameters obtained from the above described experiments and an additional ferromagnetic resonance (FMR) experiment (see Fig. 4 caption). An external magnetic field of  $8 \text{ kA m}^{-1}$  was applied normal to the film plane to tilt the magnetization towards the perpendicular direction. Initially, the bias voltage was held off (point A in Fig. 4). If we then apply a bias voltage with a slow rise time, the perpendicular anisotropy field changes and the magnetization changes its direction to point B. However, if the rise time of the pulse is short enough (less than 1 ns), a dynamic precession and switching to another energetically stable point is achieved (point C in Fig. 4). When the voltage pulse is switched off with a slow fall time, the magnetization stabilizes at point D (Fig. 4) after the relaxation process. This simulation clearly shows that if we

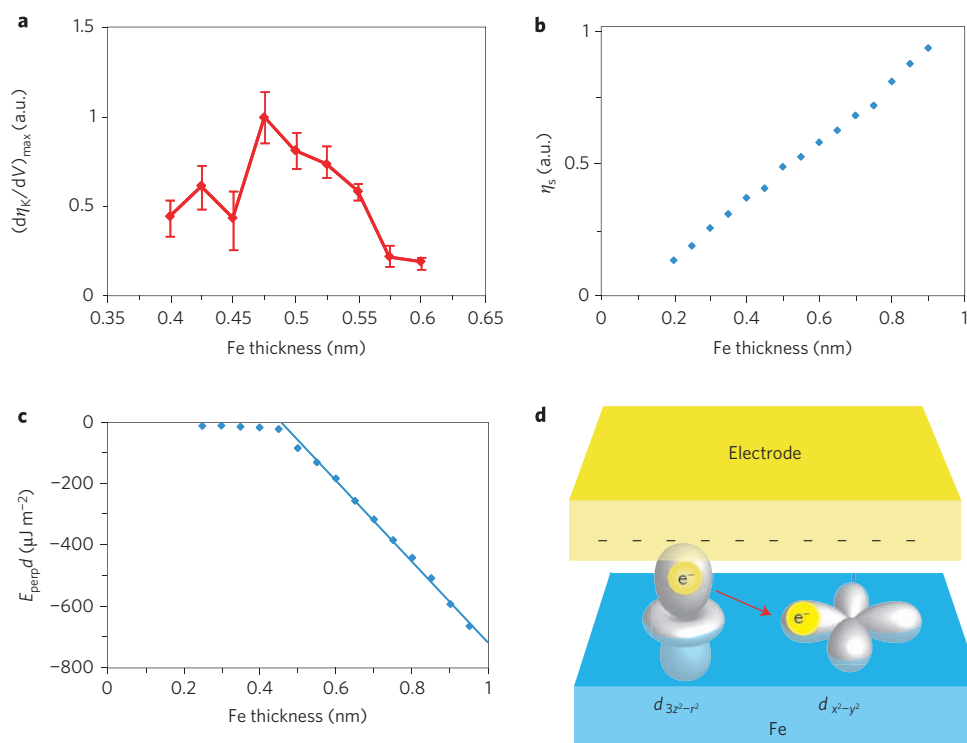


**Figure 3 | Fe layer thickness dependencies of the voltage modulation response of  $\eta_K$ , saturation Kerr ellipticity  $\eta_s$ , and  $E_{\text{perp}}d$ .** **a**, Maximum  $d\eta_K/dV$  signal as a function of Fe layer thickness. The lock-in modulation technique was used for the precise measurement of the voltage response. The line through the data is a visual aid. **b**, Fe layer thickness dependence of the saturation Kerr ellipticity  $\eta_s$ . **c**, Plot to calculate surface anisotropy energy and bulk anisotropy energy. The Y-cut corresponds to the surface anisotropy energy. The slope corresponds to the bulk anisotropy (see text). **d**, Schematic of the effect of the electric field on electron filling of the 3d orbitals in the ultrathin Fe layer. Application of a negative voltage, for example, may suppress the number of electrons in the  $m_z = 0$  states, because of the quadrupole effect.

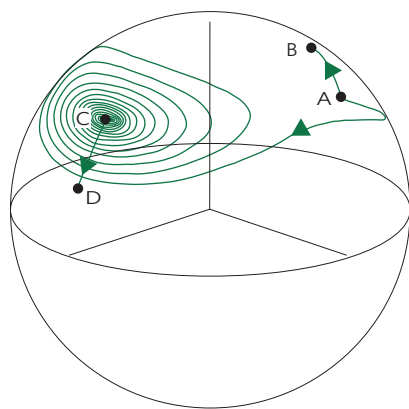


**Figure 4 | A macro spin model simulation of voltage-controlled magnetization switching.** The green line indicates the trajectory of the spin. The parameters used for the calculation include a damping constant  $\alpha = 0.025$ , perpendicular anisotropy fields of  $12 \text{ kA m}^{-1}$  for the on state and  $22 \text{ kA m}^{-1}$  for the off state. An external perpendicular field of  $8 \text{ kA m}^{-1}$  is also applied to tilt the magnetization. The magnetic cell is assumed to have a rectangular shape, with a  $1.6 \text{ kA m}^{-1}$  in-plane hard axis demagnetization field.

fabricate a Fe/MgO/Fe/Au junction with radio-frequency signal access, successful magnetization switching by the application of high-speed, low-voltage pulse should be possible. We believe that this novel magnetization switching will be demonstrated in the

near future and, by combining it with magnetoresistive structures, could prove to be a highly successful technique.

Our results show that it is possible to control magnetic anisotropy by the application of an electric field in Fe/MgO junctions, which can be combined with high-quality Fe/MgO/Fe magnetic tunnel junctions. This approach provides a technique for voltage-controlled magnetization switching and could lead to innovations in ultra-low-power spintronic devices.

## Methods

In this study, we focused on a structure comprising a solid insulator and an ultrathin epitaxial ferromagnetic layer with moderate perpendicular surface anisotropy<sup>15–20</sup>. The sample structure consisted of MgO substrate/MgO(10 nm)/Cr(10 nm)/Au(50 nm)/Fe(2–4 ML)/MgO(10 nm)/polyimide(1,500 nm)/ITO(100 nm) layers. All layers, except for the top thick polyimide and ITO layers, were grown epitaxially by a molecular beam epitaxy method, using electron beam evaporators in an ultra-high vacuum. The Au buffer layer was annealed at  $250^\circ\text{C}$ , after deposition at room temperature, to obtain an atomically flat surface. The ultrathin Fe layer and insulating MgO layer were grown on the Au(001) surface at room temperature. The sample was coated with polyimide using a spin coater, and annealed at  $200^\circ\text{C}$ . ITO was used for the top electrodes, 1 mm in diameter, and was deposited using a metal mask. A bias voltage was applied between the top ITO and the bottom Au electrode.

Magnetic hysteresis loops of ultrathin Fe films were measured using the magneto optical Kerr effect (MOKE) in a polar configuration<sup>30</sup>. The voltage dependence of the hysteresis was detected either by a direct observation of Kerr ellipticity,  $\eta_K$ , signals for different bias voltages, or by a lock-in detection of the small change in Kerr ellipticity with respect to an applied bias voltage modulation,  $d\eta_K/dV$ . The modulation amplitude and frequency were 160 V (peak-to-peak) and 37 Hz, respectively.

Received 24 June 2008; accepted 9 December 2008;  
published online 18 January 2009

## References

- Slonczewski, J. C. Current-driven excitation of magnetic multilayers. *J. Magn. Mater.* **159**, L1–L7 (1996).
- Berger, L. Emission of spin waves by a magnetic multilayer traversed by a current. *Phys. Rev. B* **54**, 9353–9358 (1996).
- Myers, E. B., Ralph, D. C., Katine, J. A., Louie, R. N. & Buhrman, R. A. Current induced switching of domains in magnetic multilayer devices. *Science* **285**, 867–870 (1999).
- Nie, X. & Blügel, S. Elektrisches Feld zur Ummagnetisierung eines dünnen Films. European patent 19841034.4 (2000).
- Duan, C.-G., Jaswal, S. S. & Tsybal, E. Y. Predicted magnetoelectric effect in Fe/BaTiO<sub>3</sub> multilayers: ferroelectric control of magnetism. *Phys. Rev. Lett.* **97**, 047201 (2006).
- Rondinelli, J. M., Stengel, M. & Spaldin, N. Carrier-mediated magnetoelectricity in complex oxide heterostructures. *Nature Nanotech.* **3**, 46–50 (2008).
- Weisheit, M. *et al.* Electric field-induced modification of magnetism in thin-film ferromagnets. *Science* **315**, 349–351 (2007).
- Chiba, D., Yamanouchi, M., Matsukura, F. & Ohno, H. Electrical manipulation of magnetization reversal in a ferromagnetic semiconductor. *Science* **301**, 943–945 (2003).
- Stolichnov, I. *et al.* Non-volatile ferroelectric control of ferromagnetism in (Ga,Mn)As. *Nature Mater.* **7**, 464–467 (2008).
- Borisov, P., Hochstrat, A., Chen, X., Kleemann, W. & Binek, C. Magnetoelectric switching of exchange bias. *Phys. Rev. Lett.* **94**, 117203 (2005).
- Chen, X., Hochstrat, A., Borisov, P. & Kleemann, W. Magnetoelectric exchange bias systems in spintronics. *Appl. Phys. Lett.* **89**, 202508 (2006).
- Chu, Y. H. *et al.* Electric-field control of local ferromagnetism using a magnetoelectric multiferroic. *Nature Mater.* **7**, 478–482 (2008).
- Eerenstein, W., Mathur, N. D. & Scott, J. F. Multiferroic and magnetoelectric materials. *Nature* **442**, 759–765 (2006).
- Novosad, V. *et al.* Novel magnetostriptive memory device. *J. Appl. Phys.* **87**, 6400–6402 (2000).
- Néel, L. Anisotropie magnétique superficielle et surstructures d'orientation. *J. Phys. Rad.* **15**, 225–239 (1954).
- Gradmann, U. Ferromagnetism near surfaces and in thin films. *Appl. Phys.* **3**, 161–178 (1974).
- Shinjo, T., Hine, S. & Takada, T. Mössbauer spectra of ultrathin Fe films coated by MgO. *Journal de Physique* **40**, C2-86–87 (1979).
- Carcia, P. F., Meinhardt, A. D. & Suna, A. Perpendicular magnetic anisotropy in Pd/Co thin film layered structure. *Appl. Phys. Lett.* **47**, 178–180 (1985).
- Gay, J. G. & Richter, R. Spin anisotropy of ferromagnetic films. *Phys. Rev. Lett.* **56**, 2728–2731 (1986).
- Liu, C. & Bader, S. D. Perpendicular surface magnetic anisotropy in ultrathin epitaxial Fe films. *J. Vac. Sci. Technol. A* **8**, 2727–2731 (1990).
- Suzuki, Y., Katayama, T., Yoshida, S. & Tanaka, K. New magneto-optical transition in ultrathin Fe(100) films. *Phys. Rev. Lett.* **68**, 3355–3358 (1992).
- Yuasa, S., Nagahama, T., Fukushima, A., Suzuki, Y. & Ando, K. Giant room-temperature magnetoresistance in single-crystal Fe/MgO/Fe magnetic tunnel junctions. *Nature Mater.* **3**, 868–871 (2004).
- Heinrich, B., Celinski, Z., Cochran, J. F., Arott, A. S. & Myrtle, K. Magnetic anisotropies in single and multilayered structures. *J. Appl. Phys.* **70**, 5769–5774 (1991).
- Bland, J. A. C. & Heinrich, B. (eds) *Ultrathin Magnetic Structures Part I*, 65–90 (Springer, 1994).
- Kyuno, K., Ha, J. G., Yamamoto, R. & Asano, S. First-principle calculation of the magnetic anisotropy energies of Ag/Fe(001) and Au/Fe(001) multilayers. *J. Phys. Soc. Jpn* **65**, 1334–1339 (1996).
- Shick, A. B., Mácá, F., Mašek, J. & Jungwirth, T. Prospect for room temperature tunneling anisotropic magnetoresistance effect: Density of states anisotropies in Cp/Pt system. *Phys. Rev. B* **73**, 024418 (2006).
- Moser, J. *et al.* Tunneling anisotropic magnetoresistance and spin–orbit coupling in Fe/GaAs/Au tunnel junctions. *Phys. Rev. Lett.* **99**, 056601 (2007).
- Gao, L. *et al.* Bias voltage dependence of tunneling anisotropic magnetoresistance in magnetic tunnel junctions with MgO and Al<sub>2</sub>O<sub>3</sub> tunnel barriers. *Phys. Rev. Lett.* **99**, 226602 (2007).
- Shick, A. B. *et al.* Tunneling anisotropic magnetoresistance in multilayer-(Co/Pt)/AlO<sub>x</sub>/Pt structures. *Phys. Rev. Lett.* **100**, 087204 (2008).
- Moog, E. R., Liu, C., Bader, S. D. & Zak, J. Thickness and polarization dependence of the magnetooptic signal from ultrathin ferromagnetic films. *Phys. Rev. B* **39**, 6949–6956 (1989).

## Acknowledgements

The authors would like to thank D. Yamaguchi, Y. Sobajima, T. Toyama and H. Okamoto for their assistance in ITO deposition. The authors also acknowledge H. Kubota, W. Van Roy, S. Blügel and T. Miyazaki for their valuable comments. A part of the research was conducted under the financial support of Grant-in-Aid for Scientific Research (A19206002) and G-COE program of Ministry of Education, Culture, Sports, Science and Technology-Japan (MEXT).

## Author contributions

Y.S. conceived and designed the experiments and performed micro magnetic calculation. T.M. and Y.S. performed the experiments and analysis. T.N. and A.A.T. led experiments and physical discussions. K.O., N.T. and M.M. established experimental techniques. S.M. and Y.A. performed FMR measurements. M.S. and T.S. contributed to general discussions. T.M. wrote the paper with review and input from Y.S., T.N. and A.A.T.

## Additional information

Supplementary Information accompanies this paper at [www.nature.com/naturenanotechnology](http://www.nature.com/naturenanotechnology). Reprints and permission information is available online at <http://npg.nature.com/reprintsandpermissions/>. Correspondence and requests for materials should be addressed to Y.S.